# Nuclear Magnetic Resonance Spectra for I > 1 Spins in Dynamically Heterogeneous Systems with Chemical Exchange Among Environments

Huiming Zhang and Robert G. Bryant
Department of Chemistry, University of Virginia, Charlottesville, Virginia 22901 USA

ABSTRACT Nuclear magnetic resonance spectra for nuclei with spin $I > 1$ are considered in cases in which the observed nucleus may sample a rotationally immobilized and an isotropic environment that are coupled by a chemical exchange process. Spectra are simulated for the central (1/2, −1/2) transition for a 3/2 nucleus as a function of the concentrations of the two environments and as a function of the exchange rate between them. It is shown that a crucial feature determining the shape of the observable spectra is the spatial extent or the local order in the immobilized phase. In the case for which all rotationally immobilized sites sampled by the exchanging nucleus are identically oriented but where there is a distribution of these microdomain orientations with respect to the magnetic field direction, a powder pattern for the central transition is observed that carries whatever dynamic information may be derived from it. In the fast exchange limit, the width of the powder pattern scales inversely with the concentration of the isotropic environment as usual. In the intermediate exchange regimes, a complex line shape results that may mask the anisotropic character of the spectrum. In the slow exchange limit, superposition of the spectral contributions results; however, if the isotropic environment concentration is significantly larger than the anisotropic environment concentration, the anisotropic contribution is very difficult to detect because of the dynamic range problem and the possibly large difference in the effective line widths. In the case for which the exchanging nucleus samples a considerable distribution of rotationally immobilized site orientations, the anisotropic character of the spectrum is lost and a super-Lorentzian line shape results. These effects are demonstrated experimentally by $^{35}Cl$ nuclear magnetic resonance spectra obtained on a lamellar liquid crystal that is modified with the addition of a thiolmercurate to provide a site of large quadrupole coupling constant and with cross-linked bovine serum albumin gels.

## INTRODUCTION

There may be considerable potential of nuclei with spin greater than 1 to provide information in dynamically heterogeneous systems. Indeed, virtually all living systems provide environments with macromolecular aggregates that reorient slowly if at all on the time scale defining rigid lattice behavior for the macromolecular spins or ions bound to macromolecules. Electrolyte ions such as sodium, potassium, and chloride ions may bind in various ways to these macromolecules or macromolecular aggregates, and their nuclear magnetic resonance (NMR) spectra may reflect these interactions (Wennerström et al., 1974; Venkatchalam and Urry, 1980; Engström et al., 1982; Forsén et al., 1987; Rooney et al., 1988; Sanders and Tsai, 1989; Wu et al., 1989; Urry et al., 1989; Rooney and Springer, 1991a,b). Most of the interactions are expected to be transient, although many may be longer lived than the time scales associated with translational diffusion. Thus, an exchange-rate and composition dependence to the spectral response of these ions is expected.

Considerable early activity in NMR of the odd-integral spins was directed at systems such as liquid crystals where there is long range order in the system (Lindman, 1983). As a result, the NMR spectra were often a powder pattern associated with the effects of first and second order quadrupole splittings that are different for different orientations of the local order director with respect to the magnetic field. In other cases, where the ordered microdomains could also be macroscopically ordered in the magnetic field such as with oriented liquid crystals, single crystal-type spectra were observed consisting of sharp lines. In their insightful review, Rooney and Springer (1991a) classify these two cases as type b and type a spectra, respectively. However, such patterns are rarely observed in tissue samples at normal levels of hydration and concentration.

Considerable recent activity has been directed at understanding in detail the NMR spectrum of sodium ion in different tissue samples, where usually the spectrum consists of a narrow and one or more broad components centered at the same frequency (Springer, 1987; Forsén et al., 1987; Urry et al., 1989; Rooney and Springer, 1991a,b). The multicomponent line, classified as a type c spectrum by Rooney and Springer (1991a), is expected if the quadrupolar spin samples environments that are in the nonextreme narrowing limit, i.e., if they experience environments where the reorientational correlation time for the electric field gradient at the observed nucleus is on the order of or longer than the reciprocal of the Larmor frequency (Hubbard, 1970; Bull, 1972; Eliav and Navon, 1990). With current NMR spectrometers, most protein binding sites are in the nonextreme narrowing regime even if the protein is free to rotate. Thus, even ions in chemical exchange with rotating proteins may fall into this category. Although rotational motions may average the first order quadrupole contributions to the spectrum, Jaccard et al. (1986) pointed out that the component contributions could be separated by passing the magnetization through states of

*Received for publication 5 July 1994 and in final form 14 March 1995.*
Address reprint requests to Dr. Robert G. Bryant, Department of Chemistry, University of Virginia, McCormick Road, Charlottesville, VA 22901. Tel.: 804-924-1494; Fax: 804-924-3710; E-mail: rgb4g@virginia.edu.

0006-3495/95/06/2556/10 $2.00

multiple quantum coherence in the acquisition process. Several groups have applied and extended this basic idea to understand more completely the line shapes and information that may be obtained from the single frequency multicomponent spectra of ions like sodium and potassium in tissues (Eliav et al., 1988; Furó et al., 1991; Stevens et al., 1992; Shinar et al., 1993; Kemp-Harper and Wimperis, 1993; Eliav and Navon, 1994). In these cases, a characteristic of the system is that the motions are sufficient to yield an effective average quadrupole resonance frequency of zero.

We address the spectroscopy from a different experimental point of view motivated by the possibility that there are advantages to observing spectra of quadrupolar ions or molecules when they are in rapid exchange with rotationally immobilized binding sites. Although there are cases when such systems may yield a single frequency multicomponent spectrum or the Rooney-Springer type c case, rotational motion of the macromolecular binding site is eliminated as a possible cause. The spectral characteristics and orientation distribution of the macromolecular environment may have major effects on the observable spectrum. Ex vivo systems that may provide rotationally immobilized environments with binding sites for observable solution phase species that may be of interest include oriented protein systems such as protein crystals, liquid crystals, or membrane-bound proteins that carry specific binding sites such as transporter enzymes. The purpose of this discussion is to examine the effects of chemical exchange rates and the character of the macromolecular orientation in the system on the observable spectral response detected by observing the labile low molecular weight species, usually an ion. The perspective is similar to that for the solution phase halide ion probe experiment (Stengle and Baldeschwieler, 1966), although the applications are more general. The model system we choose is chloride ion (Lindblom et al., 1971; Lindman and Forsén, 1976; Lindman, 1983; Suezaya et al., 1991; Lindman et al., 1992), although it is representative of other quadrupole spins to within a scale factor for the size of the quadrupole coupling constant.

The isotropic environment and the interactions with rotationally mobile macromolecules have been treated by several authors (Hubbard, 1970; Bull, 1972; Werbelow and Marshall, 1981; Werbelow and Pouzard, 1981). An important feature of these results is that, when the rotational motions slow down, the allowed transitions are no longer identical, resulting in nonexponential relaxation responses. In the case where motion in a macromolecule-bound state stops, one could record a pure nuclear quadrupole resonance spectrum because the zero-field interactions are no longer rotationally averaged. In the case where the quadrupole coupling constant may be large, as for chlorine, the resulting spectral features may be spread over tens of megahertz, making all but the central (1/2, −1/2) transition unobservable. Therefore, we focus the present discussion on observations of the (1/2, −1/2) contribution to the spectrum; however, the essence of the picture is the same for the other transitions except that the size of the exchange rates required to effect the exchange averaging of the spectrum must be larger for the much larger frequency offsets. In some cases, the exchange rates required to achieve a fast exchange-averaged powder pattern with large quadrupole coupling constants may be inaccessible.

## DEFINITION OF SYSTEMS

First we define the systems to be considered in detail based on the representations in Fig. 1. Panel (*a*) represents the situation where there is a rotationally immobilized macromolecule such as a protein with a binding site and a ligand in exchange with this binding site. This situation is distinguished from that shown in panel (*b*) where there is a single type of rotationally immobilized macromolecule with two binding sites at different orientations with respect to a molecule fixed axis system or intermediate reference frame. The ligand may exchange independently with both macromolecule sites, and the unbound sites are assumed to be dynamically isotropic environments. Neither of these limiting

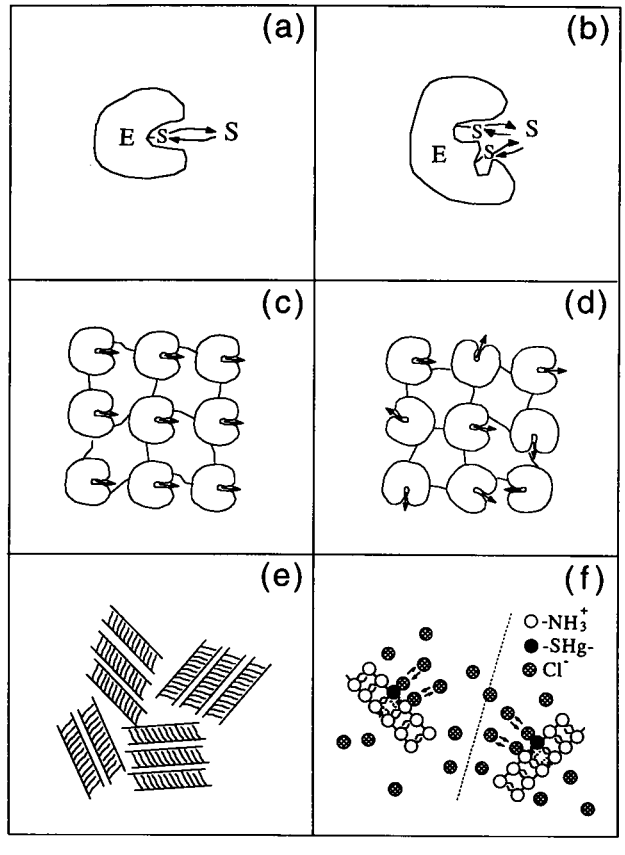


FIGURE 1 Definition of systems. (*a*) Rotationally immobilized macromolecule (E) with a binding site and a ligand (S) in exchange with this site. (*b*) Rotationally immobilized macromolecule (E) with two binding sites at different orientations with respect to an intermediate frame in exchange with a ligand (S). (*c*) An ordered array of rotationally immobilized macromolecules such that each macromolecule has the same orientation with respect to the intermediate reference frame. (*d*) Assembly of randomly oriented but rotationally immobilized macromolecules. (*e*) A liquid crystal environment where the binding sites are presumed to be on the interfacial surface. Four randomly oriented microdomains are shown. (*f*) Liquid crystal surface containing an additional component that provides a second binding site with a large anisotropic splitting.

cases is experimentally accessible; they are shown to indicate the difference between one and two binding sites that have different orientations with respect to the laboratory frame. If one could do an experiment on such a sample with sufficient sensitivity, a single crystal type spectrum would result in the fast exchange limit, but the frequency of the lines would be different because exchange is with one bound frequency in panel (*a*) but two different frequencies in panel (*b*). Panels (*c*) and (*d*) represent two important cases of macromolecular assembly that are experimentally accessible. In (*c*), the macromolecules are organized so that each molecule and associated binding site is oriented identically with respect to the intermediate fixed reference frame; in (*d*), the macromolecules are organized randomly with respect to the intermediate reference frame. In both cases, the unbound ligand is assumed to be in an isotropic environment; i.e., the ligand reorients freely and rapidly enough that the NMR spectrum is isotropic and in the extreme narrowing limit. Panel (*e*) represents the liquid crystal environment where the binding sites are presumed to be on the interfacial surface. The microdomain environment of any ligand exchanging with this surface is assumed to be uniformly oriented with respect to the intermediate reference frame, but there are four microdomains shown that are randomly oriented with respect to the laboratory frame. The observable spectrum is then a sum over contributions from these random orientations of microdomains. Panel (*f*) represents the experimental situation where we will add a new binding site to the liquid crystal surface, in addition to those associated with the counter-ion charges, that has a known and very large electric field gradient created by binding of chloride ion to mercury (II). This situation represents a sum over two interactions, the relatively weak surface binding interactions with modest quadruple coupling constants and a specific strong binding interaction with the mercury site that has a large quadruple coupling constant.

The situations we investigate are those in which the ligand of Fig. 1 carries a nucleus with spin greater than 1 and is in chemical exchange with macromolecule-bound sites that are rotationally immobilized. When bound, the ligand spin system is in the rigid lattice limit, but when unbound, dynamically it is in the extreme narrowing limit. We will investigate the character of the observable NMR spectrum of the nucleus as it is affected by the magnitude of the nuclear electric quadrupole coupling constant, the character of the orientation of the macromolecule phase, and the exchange rate of the ligand.

## EXCHANGE THEORY

The exchange master equation for each single quantum transition including chemical exchange is (Wittebort et al., 1987)

$$\dot{M} = [\mathrm{i}\tilde{\omega} + \tilde{R}]M \tag{1}$$

where M is the magnetization, $\tilde{\omega}$ is a diagonal matrix with elements that are the quadrupolar shifts at various orientations for any spin greater than 1, and $\tilde{R}$ is the jumping or exchange matrix. To obtain the contribution to the exchange matrix, $\tilde{R}$, from the enzyme-ligand reaction with isotope-labeled ligand, S, we write

$$\mathrm{E} + \mathrm{S} \underset{k_{\mathrm{off}}}{\overset{k_{\mathrm{on}}}{\Leftrightarrow}} \mathrm{ES} \tag{2}$$

where we assume that the reaction arrives at equilibrium and the binding constant, $K$, is

$$K = \frac{k_{\mathrm{on}}}{k_{\mathrm{off}}} = \frac{C_{\mathrm{ES}}}{C_{\mathrm{E}} \cdot C_{\mathrm{S}}} \tag{3}$$

where $C_i$ represents the concentration of the ith species. With the adiabatic assumption, only the transverse magnetization associated with the relevant transition is included; i.e., for the second-order quadrupolar interaction case, only the central transition is considered (Appendix). The lifetime of the free ligand is

$$\frac{1}{\tau_{\mathrm{S}}} = k_{\mathrm{on}} C_{\mathrm{E}}. \tag{4}$$

Combination with Eq. 3 yields

$$\frac{1}{\tau_{\mathrm{S}}} = k_{\mathrm{off}} \frac{C_{\mathrm{ES}}}{C_{\mathrm{S}}}. \tag{5}$$

The lifetime of the bound ligand is then

$$\frac{1}{\tau_{\mathrm{ES}}} = k_{\mathrm{off}}. \tag{6}$$

The exchange operator meets the following condition as a result of the two-site (i, j) jumping model:

$$\tilde{R}\begin{pmatrix} M^{\mathrm{i}} \\ M^{\mathrm{j}} \end{pmatrix} = \begin{pmatrix} k^{\mathrm{i}}(M^{\mathrm{i}} - M^{\mathrm{j}}) \\ k^{\mathrm{j}}(M^{\mathrm{j}} - \mathrm{M}^{\mathrm{i}}) \end{pmatrix} = \begin{pmatrix} \dot{M}^{\mathrm{i}'} \\ \dot{M}^{\mathrm{j}'} \end{pmatrix} \tag{7}$$

where $k^{\mathrm{i}}$, $k^{\mathrm{j}}$ are reciprocals of the lifetimes for species i, j; $M^{\mathrm{i}}$ and $M^{\mathrm{j}}$ are the transverse magnetizations for species $i$ and $j$, $\dot{M}^{\mathrm{i}'}$ and $\dot{M}^{\mathrm{j}'}$ represent the chemical exchange contribution to the time derivatives of $M^{\mathrm{i}}$ and $M^{\mathrm{j}}$. Thus, for the bound ligand,

$$\dot{M}^{\mathrm{ES}'} = \frac{1}{\tau_{\mathrm{ES}}}(M^{\mathrm{ES}} - M^{\mathrm{S}}) = k_{\mathrm{off}} \frac{C_{\mathrm{ES}}}{C_{\mathrm{S}}}(M^{\mathrm{ES}} - M^{\mathrm{S}}). \tag{8}$$

For the free ligand,

$$\dot{M}^{\mathrm{S}'} = \frac{1}{\tau_{\mathrm{S}}}(M^{\mathrm{S}} - M^{\mathrm{ES}}) = k_{\mathrm{off}}(M^{\mathrm{S}} - M^{\mathrm{ES}}). \tag{9}$$

If we assume that the chemical shift of the free ligand is zero, $\omega_{\mathrm{S}} = 0$, the equation of motion of the transverse magnetization for a single transition in the presence of the exchange is

$$\dot{M} = \begin{pmatrix} \mathrm{i}\omega_{\mathrm{ES}} - k_{\mathrm{off}} & k_{\mathrm{off}} \\ k_{\mathrm{off}} \dfrac{C_{\mathrm{ES}}}{C_{\mathrm{S}}} & -k_{\mathrm{off}} \dfrac{C_{\mathrm{ES}}}{C_{\mathrm{S}}} \end{pmatrix} M = (\mathrm{i}\tilde{\omega} + \tilde{R})M \tag{10}$$

where $\omega_{\mathrm{ES}}$ is the frequency of the internal interaction, i.e., the quadrupolar interaction, the chemical shielding, etc.

Thus, the transverse magnetization or the NMR signal is a function of the anisotropic splitting, the rate constants governing the equilibrium ($k_{on}$ or $k_{off}$), the concentration of the bound ligand $C_{ES}$, and the concentration of free ligand $C_S$.

To satisfy the requirement of Wittebort's diagonalization routine (Wittebort et al., 1987), we use the diagonal matrix, U, which symmetrizes the matrix $i\tilde{\omega} + \tilde{R}$:

$$U_{ij} = (P_i)^{-1/2} \tag{11}$$

where $P_i$ are the bound or free ligand populations.

To extend the development to the case where the substrate may exchange among two bound ligands, the three-site matrix becomes

$$\dot{M} = \begin{pmatrix} i\omega_1 - k_{off} & 0 & k_{off} \\ 0 & i\omega_2 - k_{off} & k_{off} \\ k_{off}\dfrac{C_{ES_1}}{C_S} & k_{off}\dfrac{C_{ES_2}}{C_S} & -k_{off}\dfrac{\sum_{i=1,2} C_{ES_i}}{C_S} \end{pmatrix} M = (i\tilde{\omega} + \tilde{R})M. \tag{12}$$

For an echo sequence $t = 2\tau$ (Wittebort et al., 1987), the magnetization equation becomes

$$M(2\tau) = \sum_{k=1} \frac{a_k}{\lambda_k - i\hat{\omega}} \sum_m a'^*_m \sum_{n=1} X_{nk} X^*_{nm} e^{(\lambda_k + \lambda^*_m)\tau}, \tag{13}$$

with

$$a_k = \sum_{i=1}^{n} \sqrt{p_i} X_i^{(k)}. \tag{14}$$

The single pulse experiment corresponds to setting $\tau = 0$. The spectral pattern is calculated as follows

$$I(\omega,\tau) = \int_0^{2\pi} \int_0^{\pi} I(\omega,\tau,\theta\phi) \sin\theta d\theta d\phi \tag{15}$$

and

$$I(\omega,\tau,\theta\phi) = Re(M) \tag{16}$$

## INTERNAL INTERACTION IN $^{35}$CL NMR

In $^{35}$Cl NMR, the chemical shielding and the second-order quadrupolar interaction contribute to the spectral pattern of the central transition. The operational Hamiltonian for the bound ligand, ES, is

$$H = H_Q + H_{CSA} \tag{17}$$

or

$$\omega = \omega_q^{(2)} + \omega_{CSA} \tag{18}$$

where $H_Q$ is quadrupolar coupling Hamiltonian, $H_{CSA}$ is chemical shielding anisotropy (CSA) Hamiltonian, $\omega_q^{(2)}$ is second-order quadrupole shift, $\omega_{CSA}$ is chemical shielding anisotropy. The expression for the corresponding resonance frequency may be derived from the second-order quadrupolar intermediate exchange theory in terms of the fourth-rank irreducible spherical tensor formalism (Zhang, 1993) (Appendix):

$$\omega_q^{(2)} = const \left( -\frac{1}{\sqrt{5}} F_0^{(0)} + 2\sqrt{\frac{2}{7}} F_0^{(2)} + \frac{9}{\sqrt{70}} F_0^{(4)} \right) \tag{19}$$

The transformation to arbitrary orientation uses the Wigner rotation matrix as usual,

$$T_m^{(l)}(\alpha\beta\gamma) = \sum_{m'} D^{(l)}_{m',-m} T_{m'}^{(l)PAS} \tag{20}$$

where the Euler angles ($\Omega_1 = \alpha\beta\gamma$) are specified relative to an intermediate frame fixed with respect to the principal axis frame of the electric field gradient tensor, or CSA tensor. This transformation generates $\omega_q^{(2)}$ for an arbitrary orientation. Then, the second rotation with Euler angles ($\Omega_2 = \theta\phi$) transforms the resultant fourth-rank tensor components, $F_0^{(l)}$ (l = 0,2,4), from the intermediate fixed frame to the laboratory frame. Thus,

$$\omega_q^{(2)}(\Omega_1,\Omega_2) = \text{const} \left( -\frac{1}{\sqrt{5}} F_0^{(0)}(\Omega_1,\Omega_2) + 2\sqrt{\frac{2}{7}} F_0^{(2)}(\Omega_1,\Omega_2) + \frac{9}{\sqrt{70}} F_0^{(4)}(\Omega_1,\Omega_2) \right), \tag{21}$$

with

$$F_0^{(l)}(\Omega_1,\Omega_2) = \sum_{m'=0,\pm1,..\pm4}^{l=0,2,4} D^{(l)}_{m'0}(\Omega_2) F_{m'}^{(l)}(\Omega_1)$$

$$F_{m'}^{(l)}(\Omega_1) = \sum_{\substack{m'=0,\pm1,..\pm4 \\ n=0,\pm2,\pm4}}^{l=0,2,4} F_n^{(l)} D^{(l)}_{nm'}(\Omega_1) \tag{22}$$

The anisotropic chemical shift is

$$\omega_{CSA} = \sqrt{\frac{2}{3}}\, \omega_0 \rho_0^{(2)}, \tag{23}$$

which, after transformation to the laboratory frame, becomes

$$\omega_{CSA}(\Omega_1,\Omega_2) = \sqrt{\frac{2}{3}}\, \omega_0 \rho_0^{(2)}(\Omega_1,\Omega_2), \tag{24}$$

with

$$\rho_0^{(2)}(\Omega_1,\Omega_2) = \sum_{m'=0,\pm1,\pm2} D^{(2)}_{m'0}(\Omega_2) \rho_{m'}^{(2)}(\Omega_1)$$

$$\rho_{m'}^{(2)}(\Omega_1) = \sum_{\substack{m'=0,\pm1,\pm2 \\ n=0,\pm2}} \rho_n^{(2)} D^{(2)}_{nm'}(\Omega_1) \tag{25}$$

$$\rho_0^{(2)} = \sqrt{\frac{3}{2}}\delta,\ \rho_{\pm1}^{(2)} = 0,\ \rho_{\pm2}^{(2)} = \frac{1}{2}\eta\delta,$$

$$\eta = \frac{\sigma_{xx} - \sigma_{yy}}{\delta},\ \delta = \sigma_{zz} - \frac{1}{3}Tr(\sigma). \tag{26}$$

## COMPUTATIONAL RESULTS

Fig. 2 summarizes the spectral patterns for the (1/2) to (−1/2) transition in two limiting cases. In both cases the composition of the system was changed from a mole fraction of 0.1 bound environment at the top of the figure to 0.9 bound at the bottom. No exchange between the environments was permitted for the spectra computed in the left panel, whereas rapid exchange at all compositions was assumed for the right panel. For both of these limiting cases no mixing of orientations was permitted by the exchange process; i.e., the spectra correspond to the cases in Fig. 1 (*c*) where there is a random distribution of microdomains of this type but no exchange between them. This situation is approximated by the schematic in Fig. 1 (*e*) where there is no exchange among the four microdomains shown, each of which may be like that in panel (*c*). The spectra shown in Fig. 2 reproduce what is expected; the slow exchange case provides a superposition of the static and the freely rotating environment spectra, but when the composition of the system is at all rich in the freely rotating component, the amplitude of the signal from the free species is so large that it is difficult to observe the immobilized component. Although this dynamic range difficulty is clearly apparent in the frequency domain presentation here, it is, in principle, less dramatic in the time domain signal at short times. The fast exchange simulations shown on the right in Fig. 2 demonstrate that the powder pattern width is proportional to the composition as expected. That is, the concentration ratio behaves as a spectral scale factor as it does in other rapid exchange cases, provided no mixing of the exchanging ligand among microdomains is permitted.

Fig. 3 displays spectra computed as in Fig. 2; however, the composition and the exchange rate between the oriented bound and the isotropic environments are changed. The fast exchange limits remain as in Fig. 2, although it is clear that the exchange between the two environments makes the line

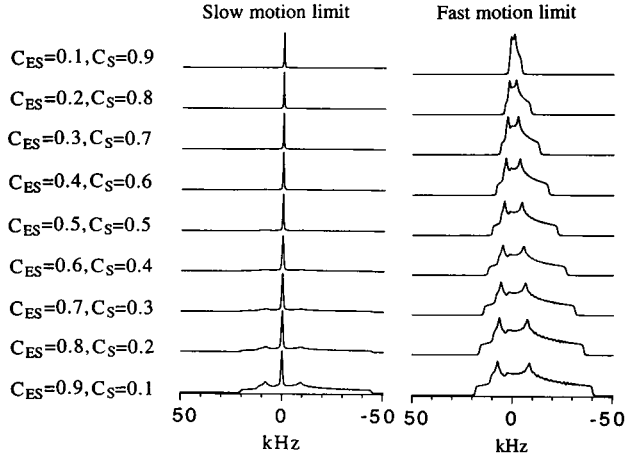


FIGURE 2 Simulated spectra for the central transition (1/2, −1/2) of a spin 3/2 nucleus in a dynamically heterogeneous environment where a bound site is rotationally immobilized and a free site is isotropic as a function of composition for the slow (left side, $k < 10^2$ Hz) and fast (right side, $k > 10^7$ Hz) exchange limit with a quadrupole coupling constant of 4 MHz and Larmor frequency of 49 MHz.

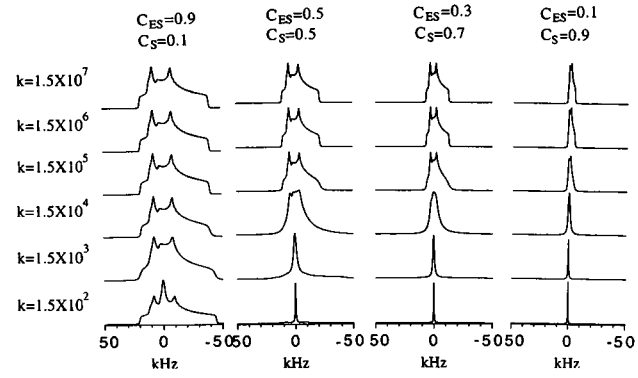


FIGURE 3 Simulated spectra for the central transition (1/2, −1/2) of a spin 3/2 nucleus in a dynamically heterogeneous environment where a bound site is rotationally immobilized and a free site is isotropic as a function of composition over a wide range of exchange rates ($10^2$ Hz < $k$ < $10^7$ Hz) with quadrupole coupling constant of 4 MHz and Larmor frequency of 49 MHz.

shape a complex function of both the composition and exchange rate. The same calculations are repeated in Fig. 4 where the quadrupole coupling constant for the bound site is increased by a factor of 3. Although the increase is only a factor of 3, the spectra have effectively shifted an order of magnitude on the exchange rate axis because the contribution of the quadrupole coupling constant enters essentially as the square.

The case represented by Fig. 1 (*b*) is shown in Fig. 5 where exchange within each microdomain is assumed to be for two bound environments that are different. Again, no mixing of microdomains is permitted so these spectra are sums over microdomain orientations; i.e., powder patterns. The simulations demonstrate that the situation rapidly becomes complex, and, with the addition of noise in an experimental spectrum, recovery of unique values for the bound site parameters would be an extremely difficult task. Nevertheless, the anisotropy of the spectra remains clear except in the cases where the exchange rates fall in the intermediate exchange domain.

These simulations demonstrate that, if one fabricated a situation like that represented in Fig. 1 (*c*), i.e., where microdomain orientation was uniform and the domain size sufficient to prevent effective mixing of the free ligand between

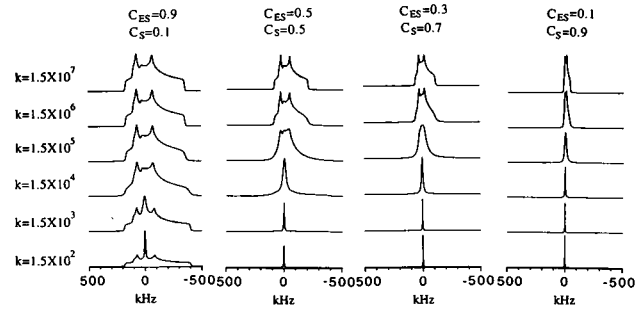


FIGURE 4 Same as Fig. 3 but with increased quadrupole coupling constant of 12 MHz.

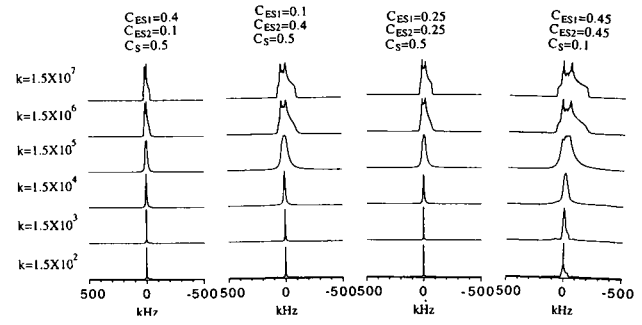


FIGURE 5 Simulated spectra for the central transition (1/2, −1/2) of a spin 3/2 nucleus in a dynamically heterogeneous environment with two different bound sites that are rotationally immobilized and a free site is isotropic as a function of composition over a wide range of exchange rates ($10^2$ Hz < $k$ < $10^7$ Hz) with quadrupolar coupling constants of 4 MHz and 12 MHz. The Larmor frequency is 49 MHz.

microdomains, then the line shape information obtained from the exchange-averaged spectra may be used together with the thermodynamic information that characterizes the binding sites to extract the bound site spectrum and what information the anisotropy of that spectrum carries, including any bound site local motional averaging. The advantage of such a situation would in principle be that the spectral width could be controlled by the composition of the system. Increasing the exchanging species concentration increases the signal-to-noise directly and also narrows the exchange-averaged spectrum, making the observation more efficient. Of course, these simulations also show that the analysis to extract the bound state spectrum is only simple in the limit of rapid exchange.

The extension of the simulation in Fig. 5 may be made either by increasing the number of different bound environments on the same enzyme or by permitting mixing among the differently oriented microdomains. The latter has been discussed previously in the context of deuterium NMR spectroscopy, and the result is generally collapse of the powder pattern to what is often called a super-Lorentzian line shape, i.e., one that is narrow at the top but very broad at the bottom (Blum et al., 1987). This is apparently also the case for most ions that have been observed in tissues (Forsén et al., 1987; Rooney et al., 1988; Urry et al., 1989; Furó, et al., 1991; Kemp-Harper and Wimperis, 1993). An experimental example will be shown in the present context for chloride ion.

## MATERIALS AND METHODS

Magnetic resonance spectra were obtained with a General Electric OMEGA-500 NMR spectrometer operating at 49.0 MHz for $^{35}$Cl. Samples were contained in 10-mm tubes and spectra recorded with a low frequency broadband probe with typical 90° pulse width of 15 μs. Bovine serum albumin (Sigma Chemical Co. A-7030, St. Louis, MO) was cross-linked with glutaraldehyde by mixing 1.6 ml of 2 mM albumin in 10 mM phosphate buffer at pH 7 with 1.3 ml of 25% aqueous glutaraldehyde (Sigma Chemical Co.) and 1.3 ml of 1.3 M NaCl or 3 M NaCl at ice temperature (Habeeb and Hiramoto, 1968). The samples were placed at 277 K overnight before measurement. The mercury derivative was prepared by adding 1.0 equivalent of mercury(II) chloride (Aldrich Chemical Co., Milwaukee, WI) to the protein before the cross-linking reaction.

The liquid crystal samples were made by dissolving $C_8H_{17}NH_3Cl$ (Eastman Kodak Co., Rochester, NY) in a water and then adding the requisite amount of decanol, which was warmed to promote dissolution (Ekwall, 1975; Lindman and Forsén, 1976; Forrest and Reeves, 1981). The sample was permitted to cool to room temperature, centrifuged for 1 h, and stored for a minimum of 2 days before measurement. The NMR spectra did not change over the period of several weeks. The presence of the lamellar phase was verified by light microscopy under crossed polarizers. The mercury derivative was obtained by adding a stoichiometric amount of mercury(II) chloride to 1-hexanethiol (Aldrich Chemical Co.) and the product dissolved in decanol before making the liquid phase. The sample compositions made are summarized in Table 1.

## LIQUID CRYSTAL RESULTS

The well characterized liquid crystal system was used for a model system to document these theoretical considerations experimentally. Fig. 6 shows the experimental $^{35}$Cl NMR spectrum of the alkyl ammonium chloride powder. The simulated spectrum is also shown where no exchange is assumed. The parameters derived from this powder pattern are used in the calculation of the exchange-averaged spectra when the liquid crystal is made from this material with water and decanol.

The $^{35}$Cl spectra of the liquid crystal are shown in Fig. 7 where the left hand column corresponds to the case of Fig. 1 (*e*) with surface sites only. The simulations of these spectra at different concentrations of chloride ion are summarized on the right side of Fig. 7 with the concentration of bound sites varying from 1 to 7% and a quadrupole coupling constant of 2.7 MHz. Rapid exchange is assumed.

The addition of a second type of site was accomplished by incorporating 0.5% of 1-hexanethiol chloromercurate, where the mercury provides a single binding site for the chloride ion when the alkyl chain is incorporated into the liquid crystal at low concentration. This type of binding site has been well characterized by much earlier work, and the ligand exchange kinetics are reported to be very rapid so that there is the best chance that the spectrum could fall into the rapid exchange limit, even though the quadrupole coupling constant for the mercury-coordinated chloride ion is expected to be between 20 and 50 MHz (Subramanian and Narasimhan, 1982; Lucken, 1969; Lindman and Forsén, 1976). Experimentally, it is clear that there is essentially no effect of the added chloromercurate sites on the detected $^{35}$Cl spectrum in the liquid crystal. This lack of effect may result from the low concentration of the alkyl mercurate species or the fact that the chloride ion exchange rate is not sufficient to provide a rapid exchange spectrum that mixes these sites significantly in this environment. Were the exchange sufficiently rapid, we would expect that the spectral widths of the middle spectra would be broader than the metal-free samples on the left,

**TABLE 1 Mole fraction compositions of liquid crystal samples**

| Sample | $C_8H_{17}NH_3Cl$ (%) | Decanol (%) | Water (%) | [$Cl^-$] (M) |
|---|---|---|---|---|
| 1 | 0.2 | 0.2 | 0.6 | 1.3 |
| 2 | 0.5 | 0.2 | 0.3 | 5 |
| 3 | 0.5 | 0.3 | 0.2 | 5 |

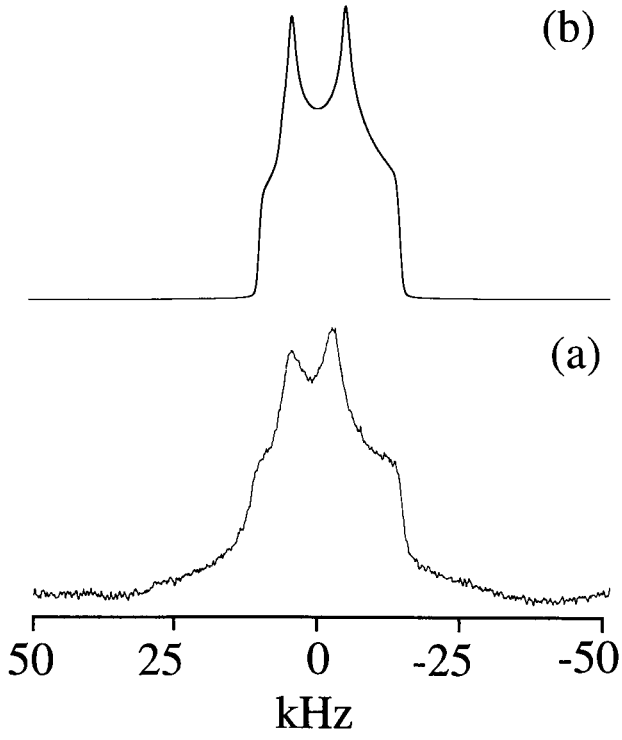


FIGURE 6 (a) $^{35}Cl$ NMR spectrum of octyl ammonium chloride powder obtained at 49 MHz. (*b*) Simulated spectrum for the central (1/2, −1/2) transition assuming an isotropic chemical shift of 60 ppm from aqueous 0.1 M aqueous sodium chloride, a quadrupole coupling constant of 2.7 MHz, an asymmetry parameter of 0.3, a CSA of 60 ppm and asymmetry factor of 1.0, and a line broadening of 100 Hz.

but they are not. Nevertheless, these samples represent an experimental example of the types represented in Fig. 1 where the orientations of the microdomains are not averaged by the exchange process.

## PROTEIN GEL RESULTS

The more common experimental situation, presumably a good model for most biological samples, is shown in Fig. 8 where a cross-linked serum albumin gel is used. As the cross-linking reaction is not orientation specific, these samples correspond to the situation in Fig. 1 (*d*). The metal-free protein gel provides a broadened chloride ion spectrum because the protein binds chloride ions with a binding affinity that is pH dependent. The line shape for the gel is super-Lorentzian. The experimental situation of Fig. 1 (*a*) that was simulated earlier with a much larger quadrupole coupling constant for one of the binding sites is provided again by the addition of mercury to the protein gel. The mercury binds readily to the sulfhydryl group of the protein and histidine groups to provide a protein-bound environment with quadrupole coupling constant in the range of 20–50 MHz (Subramanian and Narasimhan, 1982; Lucken, 1969; Lindman and Forsén, 1976). In this case, the addition of one equivalent of mercury contributes to a uniform broadening of the observable line, which retains the super-Lorentzian shape. In this case, the exchange of the chloride ion is with a number of protein molecules, each of which is randomly oriented with respect to the laboratory frame. As a consequence of the exchange averaging among rotationally immobilized sites at different orientations, the chloride ion samples many different components of the powder pattern with the result that the frequency of the chloride ion resonance is substantially averaged, the anisotropic NMR line shape is lost, and a single

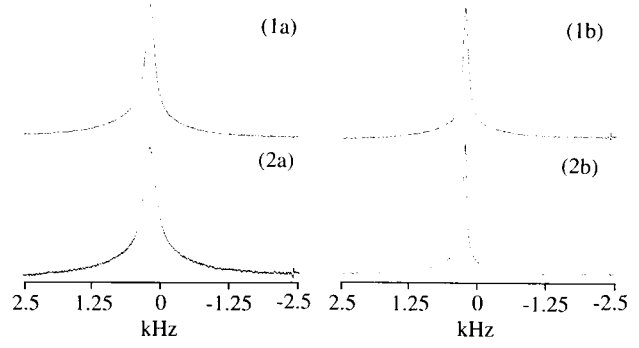


FIGURE 8 $^{35}Cl$ NMR spectra obtained at 49 MHz from a sample of 7% cross-linked bovine serum albumin (*b*) and cross-linked bovine serum albumin complex $HgCl_2$ at 1:1 ratio (*a*) in 1.3 M (*1a* and *1b*) and 3 M NaCl (*2a* and *2b*).

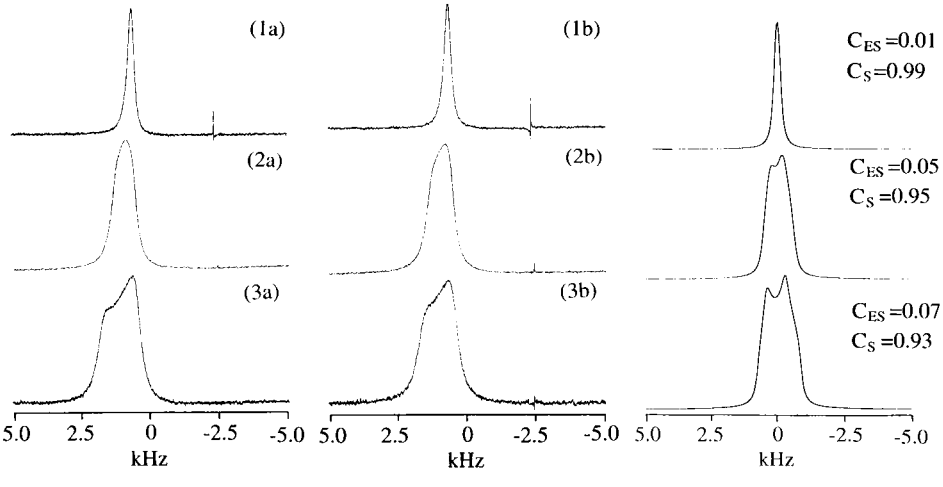


FIGURE 7 $^{35}Cl$ NMR spectra of octyl ammonium chloride-decanol-water liquid crystal system in the lamellar phase obtained at 49 MHz without (*a*) and with (*b*) 0.5% hexaylthiol-HgCl. The compositions of each sample are listed in Table 1. (*c*) Simulation of spectra with quadrupolar coupling constant of 2.7 MHz and asymmetry factor of 0.3, an isotropic chemical shift from 0.1 M aqueous sodium chloride of 60 ppm, a chemical anisotropy of 60 ppm and asymmetry factor of 1.0, and a line broadening of 100 Hz.

frequency multicomponent spectrum results. This situation corresponds to the Rooney-Springer type c spectrum found for cation resonances in many tissue samples that have been the focus of recent analyses by multiple quantum spectroscopy (Eliav and Navon, 1994; Rooney and Springer, 1991a,b).

## SUMMARY

We have examined the NMR line shape for nuclei with nuclear spin greater than 1 in the case where the nucleus may exchange between rotationally immobilized environments and a dynamically isotropic environment. When the nuclear electric quadrupole coupling constant for the nucleus is large, the width of the spectrum may be so large that only the contributions from the central (1/2, −1/2) transition generally are detected. This transition is anisotropically broadened to second and higher orders, and the anisotropy of the line shape may carry information about local dynamic averaging. If the observable nucleus may exchange between rotationally immobilized and an isotropic environment, the characteristics of the observable NMR spectrum are dependent on the nature and spatial extent of the local order of the bound or rotationally immobilized environment. In a liquid crystal-type environment where the spatial extent of the local order is large and translational motion is insufficient to cause the observed nucleus to sample different orientations of the bound sites, a powder pattern results. In the limit of rapid exchange, the observed powder pattern is simply scaled by the concentration factors as in other rapid exchange cases. As in simpler exchange cases, the line shape becomes distorted when the exchange rate is in the intermediate range; however, if the observed nucleus can sample many bound environment orientations rapidly, then the powder pattern of even the central (1/2, −1/2) transition collapses. Experimentally, this situation may be achieved by a protein gel and is the spectrum often observed in intracellular environments (Forsén et al., 1987; Urry et al., 1989).

## APPENDIX I

### Fourth-rank irreducible spherical tensor formalism for the second-order quadrupolar interaction

The second-order quadrupolar interaction that determines the central transition energy is a function of the direct products of the second-rank irreducible tensors (Abragam, 1961):

$$\Delta E^{(2)} = E^{(2)}_{1/2} - E^{(2)}_{-1/2} = -\frac{(eQ/40)^2}{\hbar\omega_0}\{32|V_{\pm 2}|^2 - 64|V_{\pm 1}|^2\}. \quad \text{(A1)}$$

To express the quadratic terms of the second-rank tensor as linear terms involving higher order tensors, we first construct the needed higher order tensors. The direct product of two irreducible tensors $T^{(l_1)}$ and $T^{(l_2)}$ is given by (Rose, 1957)

$$T^{(l_1)} \times T^{(l_2)} = \sum_{l=|l_1-l_2|}^{l_1+l_2} T^{(l)}. \quad \text{(A2)}$$

For the case at hand, $l_1 = l_2 = 2$, thus, $l$ has values of 4, 3, 2, 1, 0. Each value of $l$ has $2l + 1$ irreducible components with the following form (Rose, 1957):

$$T^{(l)}_m = \sum_{m_1,m_2} (l_1 l_2 m_1 m_2 | l_1 l_2 l m) T^{(l_1)}_{m_1} T^{(l_2)}_{m_2}$$

or

$$T^{(1)}_m = (2l+1)^{1/2} \sum_{m_1,m_2} (-l)^{-l_1+l_2-m} \begin{pmatrix} l_1 & l_2 & l \\ m_1 & m_2 & -m \end{pmatrix} T^{(l_1)}_{m_1} T^{(l_2)}_{m_2}, \quad \text{(A3)}$$

in which $\begin{pmatrix} l_1 & l_2 & l \\ m_1 & m_2 & -m \end{pmatrix}$ and $(l_1 l_2 m_1 m_2 | l_1 l_2 l m)$ are the Wigner coefficients or the vector-coupling 3j symbols (Rose, 1957; Condon and Shortley, 1935):

$$\begin{aligned} l &= l_1 + l_2, \ldots \ldots l_1 - l_2 = 4,2,0 \\ m &= \pm 4, \pm 2, 0 \\ l = 0,\ F^{(0)}_0 &= \frac{1}{4\sqrt{5}}\left(\frac{\eta^2}{3} + 1\right) V^2_{zz} \\ l = 2,\ F^{(2)}_0 &= \frac{1}{2\sqrt{14}}\left(\frac{\eta^2}{3} - 1\right) V^2_{zz} \\ F^{(2)}_{\pm 1} &= 0 \\ F^{(2)}_{\pm 2} &= \frac{1}{2\sqrt{21}}\eta V^2_{zz} \\ l = 4,\ F^{(4)}_0 &= \frac{1}{4}\sqrt{\frac{2}{35}}\left(\frac{\eta^2}{6} + 3\right) V^2_{zz} \\ F^{(4)}_{\pm 1} &= 0 \\ F^{(4)}_{\pm 2} &= \frac{1}{4\sqrt{7}}\eta V^2_{zz} \\ F^{(4)}_{\pm 3} &= 0 \\ F^{(4)}_{\pm 4} &= \frac{\eta^2}{24} V^2_{zz}. \end{aligned} \quad \text{(A4)}$$

Using these tensor components, we expand the product of the second-rank tensors as a linear combination of the fourth-rank irreducible tensors using (Rose, 1957)

$$|V^{(2)}_{\pm q}|^2 = \sum_j \begin{pmatrix} 2 & 2 & j \\ q & -q & 0 \end{pmatrix} F^{(j)}_0 \quad \text{(A5)}$$

with $j = 0, 2, 4$ and $q = 1, 2$. The result is

$$|V^{(2)}_{\pm 1}|^2 = \frac{1}{\sqrt{5}}F^{(0)}_0 - \frac{1}{\sqrt{14}}F^{(2)}_0 - \frac{4}{\sqrt{70}}F^{(4)}_0 \quad \text{(A6)}$$

$$|V^{(2)}_{\pm 2}|^2 = \frac{1}{\sqrt{5}}F^{(0)}_0 + \sqrt{\frac{2}{7}}F^{(2)}_0 + \frac{1}{\sqrt{70}}F^{(4)}_0 \quad \text{(A7)}$$

Substituting Eqs. A6 and A7 into Eq. A1, the second-order quadrupolar shift (in kHz) is

$$\nu^{(2)}_{(1/2)\leftrightarrow(-1/2)} = (-4)\frac{1}{6}\frac{(I(I+1) - 3/4)3^2}{(2I(2I-1))^2}\left(\frac{Q_{cc}{}^2}{\nu_0}\right) \left(-\frac{1}{\sqrt{5}}F^{(0)}_0 + 2\sqrt{\frac{2}{7}}F^{(2)}_0 + \frac{9}{\sqrt{70}}F^{(4)}_0\right) \quad \text{(A8)}$$

where $Q_{cc}$ is the quadrupolar coupling constant in MHz and $\nu_0$ is the Larmor frequency in MHz.

Mueller and co-workers (1991) have discussed second-order quadrupolar contributions to the spectrum. The present results are cast in irreducible form.

## Intermediate exchange theory for the second-order quadrupolar interaction

The intermediate exchange theory including the second-order quadrupolar interaction is obtained by modification of the first-order quadrupolar theory (Wittebort et al., 1987). The assumptions made for this second-order system are that the dimension of the time evolution density operator for the central transition of half integral spin $I$ is suppressed to $(2 \times 2)$ instead of $(2I + 1) \times (2I + 1)$ and includes only $m = \pm 1/2$ states:

$$\rho(t) = \begin{pmatrix} \left|\frac{1}{2}\right\rangle\left\langle\frac{1}{2}\right| & \left|\frac{1}{2}\right\rangle\left\langle-\frac{1}{2}\right| \\ \left|-\frac{1}{2}\right\rangle\left\langle\frac{1}{2}\right| & \left|-\frac{1}{2}\right\rangle\left\langle-\frac{1}{2}\right| \end{pmatrix} \tag{B1}$$

The operational Hamiltonian in the rotating frame is, therefore, reduced to $(2 \times 2)$ as well

$$H^r = \bar{H}_Q^{(0)} + \bar{H}_Q^{(1)} \tag{B2}$$

where

$$\bar{H}_Q^{(0)} = \frac{eQ}{4I(2I-1)}\sqrt{\frac{2}{3}}V_0^{(2)}(3I_z^2 - I^2) \tag{B3}$$

and

$$\bar{H}_Q^{(1)} \approx \left(\frac{e^2qQ/\hbar}{4I(2I-1)}\right)^2 \frac{1}{\omega_0}\{2(4I^2 - 8I_z^2 - 1)I_z|V_{+1}^{(2)}|^2 - 2(2I^2 - 2I_z^2 - 1)I_z|V_{+2}^{(2)}|^2\} \tag{B4}$$

In the adiabatic approximation (Wittebort et al., 1987), only the time evolution of the off-diagonal, $\rho_{1/2,-1/2}$, matrix element is considered. It obeys the equation

$$\dot{\rho}^r_{1/2,\ 1/2} = \left\langle\frac{1}{2}\right| -i[H^r_{\text{eff}},\rho^r]\left|-\frac{1}{2}\right\rangle = -i(\lambda_{1/2} - \lambda_{\ 1/2})\rho^r_{1/2,\ 1/2} \tag{B5}$$

where $\lambda_{1/2}$, $\lambda_{-1/2}$ are the energy corrections of the second-order quadrupolar interaction for states $m = +1/2$ and $m = -1/2$, $\lambda_{1/2} - \lambda_{-1/2} = \omega_q^{(2)}$, with

$$\omega_q^{(2)} = -\frac{(eQ/4\hbar)^2}{\hbar\omega_0}(32|V_{+2}|^2 - 64|V_{+1}|^2). \tag{B6}$$

Eq. 6 may be expressed in the fourth-rank irreducible spherical tensor formalism (Zhang, 1993):

$$\omega_q^{(2)} = const\left(-\frac{1}{\sqrt{5}}F_0^{(0)} + 2\sqrt{\frac{2}{7}}F_0^{(2)} + \frac{9}{\sqrt{70}}F_0^{(4)}\right) \tag{B7}$$

where

$$const = 2\pi \cdot (-4) \cdot \frac{1}{6}\frac{(I(I+1) - 3/4)3^2}{(2I(2I-1))^2}\left(\frac{Q_{cc}^{\ 2}}{\nu_0}\right). \tag{B8}$$

For the general orientation, a rotational transformation of Eq. B7, with Euler angles $(\Omega_1 = \alpha\beta\gamma)$ is specified relative to an intermediate frame fixed with respect to the principal axial frame of the electric field gradient tensor. This transformation generate $\omega_q^{(2)}$ for arbitrary orientation. A second rotation with Euler angles $(\Omega_2 = \theta\phi)$ transforms the resultant fourth-rank tensor components, $F_0^{(l)}$ $(l = 0,2,4)$, from the intermediate fixed frame to the laboratory frame. Thus,

$$\omega_q^{(2)}(\Omega_1,\Omega_2) = const\left(-\frac{1}{\sqrt{5}}F_0^{(0)}(\Omega_1,\Omega_2) + 2\sqrt{\frac{2}{7}}F_0^{(2)}(\Omega_1,\Omega_2) + \frac{9}{\sqrt{70}}F_0^{(4)}(\Omega_1,\Omega_2)\right) \tag{B9}$$

with

$$F_0^{(l)}(\Omega_1,\Omega_2) = \sum_{m'=0,\pm1,\ldots\pm4}^{l=0,2,4} D^{(l)}_{m'0}(\Omega_2)F^{(l)}_{m'}(\Omega_1) \tag{B10}$$

and

$$F^{(l)}_{m'}(\Omega_1) = \sum_{\substack{m'=0,\pm1,\ldots\pm4 \\ n=0,\pm2,\pm4}}^{l=0,2,4} F_n^{(l)} D^{(l)}_{nm'}(\Omega_1) \tag{B11}$$

The transverse magnetization is derived from the equation of motion for the spin density matrix, with interference from jumping between discrete sites, by calculating the trace of the shift operator, $M_\pm = Tr(\rho I_\pm)$, as well as $M_\pm = \text{Tr}(\dot{\rho}I_\pm)$. Thus, we obtain an equation similar to Eq. 3.4 in Wittebort's paper (Wittebort et al., 1987), in which the matrix $\omega$ is replaced with one calculated from the second-order quadrupolar shifts, $\omega_q^{(2)}$, rather than first-order splitting:

$$\dot{M}^i = \sum_{j=1}^{N}(-i\omega^{(2)}(\Omega_1,\Omega_2)\delta_{ij} + R_{ij})M^j. \tag{B12}$$

This work was supported by National Institutes of Health grant SR01-GM36796.

## REFERENCES


Abragam, A. 1961. The principals of nuclear magnetism. The University Press, Claredon. 233–234.

Blum, F. D., E. I. Franses, K. D. Rose, R. G. Bryant, and W. G. Miller. 1987. Structure and dynamics in lamellar liquid crystals: effect of agitation and aging on deuterium NMR line shapes. *Langmuir* 3:448–452.

Brown, R. J., B. K. Hunter, M. Mackowiak, and S. Segel. 1982. Relaxation in calcium hexachlorostannate hexahydrate. *J. Magn. Reson.* 50:218–226.

Bull, T. E. 1972. Nuclear magnetic relaxation of spin-2/3 nuclei involved in chemical exchange. *J. Magn. Reson.* 8:344–353.

Condon, E. U., and G. H. Shortley. 1935. The Theory of Atomic Spectra. The University Press, New York.

Ekwall, P. 1975. Composition, properties and structures of liquid crystalline phases in system of amphiphilic compounds. *Adv. Liquid Cryst.* 1:1–141.

Eliav, U., A. Baram, and G. Navon. 1988. Nuclear magnetic resonance line shapes of exchanging spin 3/2 nuclei. *J. Chem. Phys.* 89:5584–5588.

Eliav, U., and G. Navon. 1990. Criteria for multiexponential relaxation of exchanging spin 3/2 nuclei. *J. Magn. Reson.* 88:223–240.

Eliav, U., and G. Navon. 1994. Analysis of double quantum filtered NMR spectra of $^{23}$Na in biological tissues. *J. Magn. Reson. B.* 103:19–29.

Engström, S., B. Jöhnsson, and B. Jöhnsson. 1982. A molecular approach to quadrupole relaxation: Monte Carlo simulations of dilute $Li^+$, $Na^+$, and $Cl^-$ aqueous solutions. *J. Magn. Reson.* 50:1–20.

Forrest, B. J., and L. W. Reeves. 1981. New lyotropic liquid crystals composed of finite nonspherical micelles. *Chem. Rev.* 81:1–14.

Forsén, S., T. Drakenberg, and H. Wennerström. 1987. NMR studies of ion binding in biological systems. *Q. Rev. Biophys.* 19:83–114.

Furó, I., B. Halle, and L. Einarsson. 1991. Methods for NMR studies of I > 1 nuclei in anisotropic systems with small quadrupole splitting. *Chem. Phys. Lett.* 182:547–550.

Habeeb, A. F. S. A., and R. Hiramoto. 1968. Reaction of proteins with glutaraldehyde. *Arch. Biochem. Biophys.* 126:16–26.

Hubbard, P. S. 1970. Non-exponential nuclear magnetic relaxation by quadrupolar interactions. *J. Chem. Phys.* 53:985–987.

Jaccard, G., S. Wimperis, and G. Bodenhausen. 1986. Multiple quantum NMR spectroscopy of S = 3/2 spins in isotropic phase: a new probe for multiexponential relaxation. *J. Chem. Phys.* 85:6282–6293.

Kemp-Harper, R., and S. Wimperis. 1993. Detection of the interaction of sodium ions with ordered structures in biological systems: use of the Jeener-Broekaert experiment. *J. Magn. Reson. B.* 102:326–331.

Larsson, K. M., J. Kowalewski, and U. Henriksson. 1985. A multinuclear approach to molecular dynamics in dichloromethylsilane and related compounds. *J. Reson. Magn.* 62:260–268.

Lindblom, G., H. Wennerstöm, and B. Lindman. 1971. Ion binding in liquid crystals studied by NMR. II. $^{35}Cl$ second-order quadrupole interactions in a lamellar mesophase. *Chem. Phys. Lett.* 8:489–492.

Lindman, B. 1983. Amphiphilic and polyelectrolyte systems. *In* NMR of Newly Accessible Nuclei, Vol. 1. P. Laszlo, editor. Academic Press, New York. 193–231.

Lindman, B., and S. Forsén. 1976. Chlorine, Bromine and Iodine NMR: Physico-Chemical and Biological Applications. Springer-Verlag, New York.

Lindman, B., H. Wennerström, and S. Forsén. 1992. Halide ion quadrupolar relaxation in aqueous solutions containing organic cations. *J. Phys. Chem.* 96:5669–5670.

Lucken, E. A. C. 1969. Nuclear Quadrupole Coupling Constants. Academic Press, New York.

Mueller, K. T., Y. Wu, B. F. Chmelka, J. Stebbins, and A. Pines. 1991. High-resolution oxygen-17 NMR of solid silicates. *J. Am. Chem. Soc.* 113:32–38.

Rooney, W. D., T. M. Barbara, and C. S. Springer, Jr. 1988. Two-dimensional double-quantum NMR spectroscopy of isolated spin 3/2 systems: $^{23}Na$ examples. *J. Am. Chem. Soc.* 110:674–681.

Rooney, W. D., and C. S. Springer, Jr. 1991a. A comprehensive approach to the analysis and interpretation of the resonances of spins 3/2 from living systems. *NMR Biomed.* 4:209–226.

Rooney, W. D., and C. S. Springer, Jr. 1991b. The molecular environment of intracellular sodium: $^{23}Na$ NMR relaxation. *NMR Biomed.* 4:227–245.

Rose, M. E. 1957. Elementary Theory of Angular Momentum. John Wiley & Sons, New York.

Sanders, C. R. II, and M.-D. Tsai. 1989. Ligand-protein interactions via nuclear magnetic resonance of quadrupolar nuclei. *Methods Enzymol.* 177:317–333.

Suezaya, H., N. Horiike, S. Yamazaki, H. Kamachi, and M. Hirota. 1991. Multinuclear NMR spectroscopic studies on ionic interactions: interactions between nitrogen cations and halide ions. *J. Phys. Chem.* 95:10787–10796.

Shinar, H., T. Knubovets, U. Eliav, and G. Navon. 1993. Sodium interaction with ordered structures in mammalian red blood cells detected by Na-23 double quantum NMR. *Biophys. J.* 64:1273–1279.

Springer, C. S. 1987. Measurement of metal cation compartmentation in tissue by high-resolution metal cation NMR. *Annu. Rev. Biophys. Biophys. Chem.* 16:375–399.

Stengle, T. R., and J. D. Baldeschwieler. 1966. Halide ions as chemical probes for nuclear magnetic resonance studies of proteins. *Proc. Natl. Acad. Sci. USA.* 55:1020–1025.

Stevens, A., P. Paschalis, and T. Schleich. 1992. Sodium-23 and potassium-39 nuclear magnetic resonance relaxation in eye lens: examples of quadrupole ion magnetic relaxation in a crowded protein environment. *Biophys. J.* 61:1061–1075.

Subramanian, V. H., and P. T. Narasimhan. 1982. $^{35}Cl$ powder Zeeman NQR studies using an injection- and phase-locked NQR spectrometer. *J. Mol. Struct.* 58:193–203.

Urry, D. W., T. L. Trapane, C. M. Venkatachalam, and R. B. McMichens. 1989. Ion interactions at membranous polypeptide site using nuclear magnetic resonance: determining rate and binding constants and site locations. *Methods Enzymol.* 171:287–342.

Venkatchalam, C. M., and D. W. Urry. 1980. Analysis of multisite ion binding using sodium-23 NMR with application to channel-forming micellar-packaged malonyl gramicidin. *J. Magn. Reson.* 41:313–335.

Wennerström, H., G. Lindblom, and B. Lindman. 1974. Theoretical aspects on the NMR of quadrupolar ionic nucli in micellar solutions and amphiphilic liquid crystals. *Chemica Scripta.* 6:97–103.

Werbelow, L. G., and A. G. Marshall 1981. The NMR of spin-3/2 nuclei: the effect of second order dynamic frequency shifts. *J. Magn. Reson.* 43:443–448.

Werbelow, L. G., and G. Pouzard 1981. Quadrupolar relaxation. The multiquantum coherences. *J. Phys. Chem.* 85:3887–3891.

Wittebort, R. J., E. T. Olejiniczak, and R. G. Griffin. 1987. Analysis of deuterium nuclear magnetic resonance line shapes in anisotropic media. *J. Chem. Phys.* 86:5411–5420.

Wu, Y., T. M. Barbara, W. D. Rooney, and C. S. Springer, Jr. 1989. Two-dimensional multiple-quantum NMR spectroscopy of isolated half-integer spin systems. II. $^{35}Cl$ examples. *J. Magn. Reson.* 83:279–298.

Zhang, H. 1993. Solid state $^{17}O$ NMR studies of hydrate in biomolecules and $^{2}H$ NMR studies of chain dynamics in crystalline $[Cd(CH_3CH_2CH_2CH_2NH_3)_2]Cl_2$. Ph.D. thesis. University of Louisville, Louisville, KY.